Designing, Generating and Reconfiguring Disclination Interconnects in Nematic Liquid Crystals

Miao Jiang [a, †], Yubing Guo [b, †], Robin L B Selinger[c,d], Oleg D Lavrentovich[c,d], Qi-Huo Wei [a, d, e*]

[a] *Department of Mechanical and Energy Engineering, Southern University of Science and Technology, Shenzhen 518055, China*

[b] *School of Medical Technology, Beijing Institute of Technology, Beijing 100081, China*

[c] *Advanced Materials and Liquid Crystal Institute, and Department of Physics, Kent State University, Kent, OH 44242, USA*

[d] *Department of Physics, Kent State University, Kent, OH 44242, USA*

[e] *Center for Complex Flows and Soft Matter Research, Southern University of Science and Technology, Shenzhen 518055, China*

[†] Equal contribution

[*] Correspondence to: weiqh@sustech.edu.cn

Disclinations in nematic liquid crystals are of great interest both theoretically and practically. The ability to create and reconfigure disclinations connecting predetermined points on substrates could enable novel applications such as directed self-assembly of micro/nanoparticles and molecules. In this study, we present a novel approach to design and create disclination interconnects that connect predetermined positions on substrates. We demonstrate that these interconnects can be switched between different states by re-writing photoalignment materials with linearly polarized light, and can be switched between degenerate states using electric fields.

Keywords: nematic liquid crystal; disclination; molecular photopatterning; reconfiguration

1. Introduction

Nematic liquid crystals exhibit rich topological structures that cannot be eliminated by continuous rotations of the molecular orientations, i.e., the director [1–4]. One common example is the disclination, which is a line defect of singularity in the director field. The director along a closed loop around the disclination rotates multiple times of π [5], and the strength of the disclination (k) is defined as the number of 2π rotations of director ($\Delta\theta$) around the line, i.e., $k = \Delta\theta/2\pi$. Nematic liquid crystals with engineered disclinations can find important applications, such as photonic applications [6–9], command of active matters [10,11], programmed shape-morphing [12,13], and directed self-assembly [14–16].

These intriguing applications have inspired significant research efforts in creating designable disclinations in nematic liquid crystals [17–20]. Designer disclinations can be induced by colloids and their aggregates with different topologies. For example, dispersed spherical colloid particles with perpendicular surface anchoring can form elastic dipole or Saturn-ring shape disclination in nematic liquid crystal [18]. Array of spherical colloids can induce knots and links of disclinations [21]. Nonspherical colloids with lower symmetry or different topologies can further enrich disclination states [22]. Disclinations created around colloidal particles can be reconfigured between degenerate states through electric fields, photothermal melting and laser tweezing[23–25]. Disclinations can also be generated by geometric boundaries and surface microstructures. A well-known structure is a disclination in a tube with perpendicular surface alignment. Another example is disclination rings pinned to a microfiber, which can be created and manipulated with light illumination [26]. Microstructures, such as air pillars, provide the possibility to creating and to controlling the defects around them [27]. Additional disclinations can be generated by carefully designed alignment patterns on opposite confining surfaces of the liquid crystal cells. These disclinations can be reconfigured by an external electric field [28]. Disclination webs can also be generated by designing alignment patterns on liquid crystal cell surfaces [29] . In a previous work, a strategy was developed to precisely create complex 3D disclination networks by freely designing surface alignment patterns with the plasmonic photopatterning technique [30–33]. We demonstrated suspended disclination interconnects with designer polygonal shapes and anchored disclination networks connecting desired sites on two confining surfaces. We further exhibited the capability to control the curvature, size, and shape of these disclinations by changing one surface alignment pattern [30].

Recently, the reconfiguration of disclinations, including changing disclination shapes and changing disclination network connections between two bistable states, was realized through light illumination [34,35], electric field [28,36,37] or laser tweezer [26,38]. These exciting works presented certain reconfigurations of disclinations, exhibited the dynamics of the disclinations manipulation, and enabled dynamic control of self-assembled colloidal particles and quantum dots. For example, Cipparrone et al. demonstrated manipulation of quantum dots assembled disclinations by optical tuning of cholesteric LC pitch [34], Yoshida et al. exhibited reconfiguration of disclinations and colloidal particle positions by an external electric field [28].

Here, we present a versatile approach to design and create disclinations that interconnect predetermined spots on flat substrates and to optically switch disclination interconnects between different topological states by using the rewritable property of photoalignment materials and applying electric fields. Using a plasmonic photopatterning technique, we can align liquid crystal molecules at the top and bottom surfaces into orientation patterns with topological defects of different topological charges and lattice structures, leading to disclinations that interconnect these defects at substrate surfaces. By optically rewriting the alignment director fields at the top and bottom surfaces, we can switch disclinations between interconnecting two surfaces and one surface and between interconnecting along different orientations. We show that degenerate states of disclinations can be switched by applying external electric fields. These demonstrated reconfiguration capabilities make it possible to precisely design, generate, and reconfigure three-dimensional disclination interconnects, enabling new approaches in various applications, such as transporting self-assembling nano/micro-particles and sorting in microfluidic applications.

2. Experimental Methods

2.1. Liquid crystal cell fabrication

The glass substrates were prepared for surface functionalization by cleaning with isopropanol and acetone, followed by exposure to UV ozone for 10 minutes to enhance surface hydrophilicity. The substrates were then spin-coated with a 0.5wt% solution of brilliant yellow (BY) in dimethylformamide at a speed of 1500 rpm for 40 seconds, and baked on a hot plate at 90℃ for 30 minutes. Orientation patterns encoded in plasmonic metamasks were photo-imprinted onto the

BY molecules using methods previously described in literature [31-33]. To fix these molecular orientation patterns, the substrates were coated with a toluene solution of 0.5wt% photoinitiator irgacure 651 (from ciba) and 10wt% reactive mesogen 257 (RM257, EM industry) at a speed of 3000 rpm for 40 seconds, followed by exposure to nonpolarized UV light with a wavelength of 365 nm to induce photo-polymerization.

Two substrates imprinted with the predesigned orientation patterns were assembled to form a liquid crystal cell and then filled with liquid crystals in their isotropic phase. The cell thickness was controlled using 5 μm spacers. Electric fields were applied by patterning glass substrates coated with indium tin oxide (ITO) films using standard photolithography. The ITO was subsequently etched using wet chemistry to yield ITO electrodes on the glass substrates.

2.2. Disclination Reconfiguration

In the optical reconfiguration experiments, a linearly polarized white light (X-cite series 120) with an intensity of approximately 100 mW/cm^2 was used. The light was directed onto the top surface of the LC cells to rewrite the alignment pattern on that surface. The reconfiguration process was recorded using a CCD camera under a cross-polarized microscope or bright field microscope. For the electric field-driven reconfiguration, an electric field with an amplitude of 0.3 V/μm and a frequency of 3000 Hz was applied.

3. Results and discussion

3.1. Design and generation of disclination interconnects

To demonstrate the controllability and versatility of our engineering approach in generating pre-designed disclinations interconnecting substrates, we have developed three representative examples. In our previous work, we presented the details of our approach, which is based on photopatterning molecular orientations at two confining flat surfaces to create 2D orientation fields containing topological defects [30]. This approach takes advantage of the fact that line defects cannot end in the bulk and must either form loops in the bulk or end at interfaces. By patterning confining surfaces with such orientation fields, we can generate disclinations that connect these defect cores, which can be on the same confining substrate or on two opposite sides of the liquid crystal cells.

The first example involves generating disclination networks with ±1 defect arrays on the bottom confining surface and uniform alignment on the top confining surface, as illustrated in Figure 1a. The director orientational angle, θ, on the bottom surface is defined as a linear function of the azimuthal angle φ: $\theta = k\varphi + \theta_0$, where k represents the topological charge and is either +1 or -1 in this case, and θ_0 is the initial angle when $\varphi = 0°$. Typically, each +1 or -1 defect separates into two +1/2 and/or -1/2 defects to minimize the free energy, as the elastic energy of a disclination is proportional to k^2. Consequently, we observe two disclinations around each defect center, as shown in Figure 1b. By varying the orientation of the uniform alignment on the top surface, we can control the radius of curvature and connecting direction of the disclinations, as depicted in Figures 1c-f.

In the second example, we demonstrate that the number of disclinations emitted from each defect center is controllable by varying the topological charges of the defects in the bottom surface alignment. We utilized an array of ±3 topological defects, which initiate six disclination lines anchored around each defect center, as illustrated in Figure 2a-b. By using defect arrays with ±n topological charge, we can create disclination interconnects with 2n disclination lines anchored around each defect center. Similar to the first example, we can manipulate the radius curvature and connecting direction of these disclinations by varying the top surface uniform alignment.

The third example showcases the designability of the lattice of disclination networks, which can take on any lattice. In the previous examples, we utilized a square lattice of defect arrays on the bottom surface. However, by replacing the bottom surface patterns with a hexagonal lattice of +1 defect arrays (red spots in Figure 3a), we observed a hexagonal lattice of disclination networks (Figure 3b). Each +1 defect center anchors two disclination lines, whereas each -1/2 defect center (green spots in Figure 3a) anchors only one disclination line. Interestingly, when the top surface uniform alignment has an orientational angle of θ=30° (Figure 3c), the disclination lines anchored on +1 defect centers can connect either with the -1/2 defect center along the x-direction or with the -1/2 defect center at different rows. Again, the radius curvature and connecting direction of these disclination networks can be manipulated by varying the top surface uniform alignment.

3.2. Optical reconfiguration of disclinations

Reconfiguration of disclination interconnects can be achieved by taking advantage of the rewritability of azo-dye photoalignment material. Specifically, the alignment pattern on bounding

surfaces can be changed to a new one via illuminating light with specific polarization patterns. In this study, plasmonic photopatterning was utilized to encode the designed liquid crystal alignment patterns on both the top and bottom substrate surfaces, and the bottom surface alignment pattern was locked by spin-coating and photopolymerization of a thin layer of 4-(3-Acryloyloxypropyloxy) benzoic acid 2-methyl-1,4-phenylene ester (RM257). A cell was assembled with patterned top and bottom substrates, and E7 was filled into the cell by capillary force. Then, polarized light was used to illuminate the cell from the top surface to rewrite the alignment pattern on that surface. As demonstrated in Figures 4 and 5, disclination interconnects can be optically reconfigured between different states. Due to the excellent rewritability of azo-dye, disclinations can be reversibly reconfigured with sufficient exposure time.

3.2.1. Switching between interconnecting two surfaces and one surface

We first explored the capability of switching disclination interconnects from connecting two surfaces to connecting only one surface. We started with a cell having the same ±1 defect arrays on both top and bottom surfaces, as schematically shown in the top row of Figure 4a. Each defect separated into two half defects, and each disclination connected defects with the same topological charge on different surfaces. Since these disclinations are approximately along the z-axis, they are hardly visible under cross-polarized microscopy (Figure 4b). We illuminated the sample with linearly polarized light to convert the top surface alignment from a patterned director into a uniform director along the x-axis, as schematically shown in the bottom row of Figure 4a. In this case, there is no defect on the top surface, and disclinations can only connect defect centers on the bottom surface. From cross-polarized microscopy imaging (Figure 4c), we observed that these disclinations connected defect centers with opposite topological charges along the y-axis.

The switching process was recorded with a bright-field optical microscope and presented in Figure 4d-k. At the beginning, we see two dots around each defect center, corresponding to two disclinations approximately along the z-axis. Around 80 seconds after illumination with linearly polarized light, these dots grow larger because the top ends of these disclinations move away from the defect cores and curve toward the bottom surface. These disclinations continue to grow and then two neighboring disclinations reconnect and form a new one connecting two defect centers with opposite topological charges on the bottom surface. The reconfiguration process takes 300 to 360 seconds. Since two original disclinations recombine into a new one, the number of

disclinations is reduced by half, which agrees with the fact that the number of defect centers is reduced by half due to the conversion of the top surface alignment from ±1 defect arrays to uniform alignment. The detailed process of the recombination of two disclination lines into a new one is interesting and still needs further experimentation or simulations.

3.2.2 Switching between interconnecting defect centers of different orientations

We investigated the reconfiguration of disclination networks to connect neighboring centers of topological defects with opposite topological charges along a different axis, as shown in Figure 5a. The bottom substrate coated with the BY alignment film was photo-patterned with orientation fields of ±1 defect array and then coated with a thin film of RM257, which was photopolymerized in vacuum to fix the director patterns. The top surface was photo-patterned to form a uniform alignment along the y-axis with brilliant yellow only. Disclination lines were observed to connect neighboring centers of topological defects with opposite topological charges along the x-axis (Figure 5b). Illumination of the sample with light linearly polarized along the y-axis converted the uniform alignment on the top surface from along the y-axis to along the x-axis, and after reconfiguration, disclination lines connected defect centers with opposite topological charges along the y-axis (Figure 5c).

We recorded bright field microscope images of the liquid crystal cell during the conversion process and showed them in Figure 5d-k. During this process, the disclinations first grew longer against line tension and gradually bent to get close to their neighboring ones (Figure 5e). Two disclinations reconnected and then separated into new disclinations connecting defect centers along the y-axis. The separation process was fast, taking less than 0.05 seconds. Finally, these new disclinations gradually changed into short lines along the y-axis, which agreed with the new surface alignment patterns.

3.3. Switching between two degenerate states

As schematically shown in Figure 6a, when the director on the top surface is oriented at 45 degrees, disclinations interconnecting ±1 defect centers along the x-axis and y-axis are two degenerate states with the same elastic free energy. The corresponding cross-polarized microscope images are presented in Figure 6b. We found that these two degenerate states can be switched into each other by applying an external electric field along the y-axis or x-axis.

In Figure 6d-i, we present one such reconfiguration process. We selected a liquid crystal cell with disclination interconnects connecting defect centers along the y-axis and applied an electric field with a magnitude of 0.3V/μm along the y-axis. We observed that all disclinations were dragged in the -x direction at different speeds. Specifically, disclinations originally curved in the -x direction deformed much faster than those originally curved in the +x direction (Figure 6e-f). One faster deformed disclination met with another slower deformed disclination, and then they immediately separated to form two new disclinations connecting defect centers along the x-axis (Figure 6g-i). We remark that due to the fast response of liquid crystal molecules to external electric field, we can reversibly reconfigure disclinations into different degenerate states.

4. Conclusions

We have presented a versatile approach for designing disclinations that interconnect topological defects at flat surfaces, and demonstrated how to generate them using the plasmonic photopatterning technique to create pre-designed molecular orientations at two flat surfaces. Moreover, we have showcased the ability to optically reconfigure disclination networks through two representative examples: switching disclinations between connecting defects at two surfaces, and at one surface, switching disclinations between connecting defect centers along the x-axis to along the y-axis. Additionally, we have shown that disclination interconnects with two degenerate states can be switched by applying an external electric field. We anticipate that these capabilities will offer dynamic control in various applications, including the directed self-assembly of micro-/nano-particles, photonic applications, and control of active matters.

Disclosure statement

No potential conflict of interest was reported by the authors.

Funding

This work was supported by Shenzhen Science and Technology Innovation Committee GJHZ-20200731095212036, National Natural Science Foundation of China 6210030761 and 12174177.

References

[1] de Gennes PG, Prost J, Pelcovits R. *The Physics of Liquid Crystals*. Phys Today. 1995;48:70–71.

[2] Jagodzinski H. *Points. lines and walls in liquid crystals, magnetic systems and various ordered media* by M. Kléman. Acta Crystallogr A. 1984;40:309–310.

[3] Alexander GP, Chen BG, Matsumoto EA, et al. *Colloquium* : Disclination loops, point defects, and all that in nematic liquid crystals. Rev Mod Phys. 2012;84:497–514.

[4] M. Kleman, Lavrentovich OD, Nastishin YAYA. Dislocations and Disclinations in Mesomorphic Phases. Dislocations in Solids 2004 p. 147–271.

[5] Ishikawa T, Lavrentovich OD. Crossing of disclinations in nematic slabs. Europhys Lett. 1998;41:171–176.

[6] Marrucci L, Manzo C, Paparo D. Optical spin-to-orbital angular momentum conversion in inhomogeneous anisotropic media. Phys Rev Lett. 2006;96:163905.

[7] Marrucci L, Karimi E, Slussarenko S, et al. Spin-to-orbital conversion of the angular momentum of light and its classical and quantum applications. Journal of Optics. 2011;13:064001.

[8] Wei BY, Hu W, Ming Y, et al. Generating switchable and reconfigurable optical vortices via photopatterning of liquid crystals. Adv Mater. 2014;26:1590–1595.

[9] Čančula M, Ravnik M, Žumer S. Generation of vector beams with liquid crystal disclination lines. Phys Rev E. 2014;90:022503.

[10] Peng C, Turiv T, Guo Y, et al. Command of active matter by topological defects and patterns. Science. 2016;354:882–885.

[11] Turiv T, Krieger J, Babakhanova G, et al. Topology control of human fibroblast cells monolayer by liquid crystal elastomer. Sci Adv. 2020;6:eaaz6485.

[12] Ware TH, McConney ME, Wie JJ, et al. Voxelated liquid crystal elastomers. Science. 2015;347:82–984.

[13] Babakhanova G, Turiv T, Guo Y, et al. Liquid crystal elastomer coatings with programmed response of surface profile. Nat Commun. 2018;9:456.

[14] Wang X, Miller DS, Bukusoglu E, et al. Topological defects in liquid crystals as templates for molecular self-assembly. Nat Mater. 2016;15:106–112.

[15] Lee E, Xia Y, Ferrier RC, et al. Fine Golden Rings: Tunable Surface Plasmon Resonance from Assembled Nanorods in Topological Defects of Liquid Crystals. Adv Mater. 2016;28:2731–2736.

[16] Fleury JB, Pires D, Galerne Y. Self-Connected 3D architecture of microwires. Phys Rev Lett. 2009;103:267801.

[17] Smalyukh II. Review: knots and other new topological effects in liquid crystals and colloids. Rep Prog Phys. 2020;83:106601.

[18] Gu Y, Abbott NL. Observation of Saturn-Ring Defects around Solid Microspheres in Nematic Liquid Crystals. Phys Rev Lett. 2000;85:4719–4722.

[19] Lapointe CP, Mason TG, Smalyukh II. Shape-Controlled Colloidal Interactions in Nematic Liquid Crystals. Science. 2009;326:1083–1086.

[20] Poulin P. Novel Colloidal Interactions in Anisotropic Fluids. Science. 1997;275:1770–1773.

[21] Poulin P, Stark H, Lubensky TC, et al. Novel colloidal interactions in anisotropic fluids. Science. 1997;275:1770–1773.

[22] Čopar S, Tkalec U, Muševič I, et al. Knot theory realizations in nematic colloids. Proc Natl Acad Sci U S A. 2015;112:1675–1680.

[23] Lapointe CP, Mason TG, Smalyukh II. Shape-Controlled Colloidal Interactions in Nematic Liquid Crystals. Science. 2009;326:1083–1086.

[24] Martinez A, Ravnik M, Lucero B, et al. Mutually tangled colloidal knots and induced defect loops in nematic fields. Nat Mater. 2014;13:258–263.

[25] Senyuk B, Liu Q, He S, et al. Topological colloids. Nature. 2013;493:200–205.

[26] Nikkhou M, Škarabot M, Čopar S, et al. Light-controlled topological charge in a nematic liquid crystal. Nat Phys. 2015;11:183–187.

[27] Kim DS, Čopar S, Tkalec U, et al. Mosaics of topological defects in micropatterned liquid crystal textures. Sci Adv. 2018;4:eaau8064.

[28] Yoshida H, Asakura K, Fukuda J, et al. Three-dimensional positioning and control of colloidal objects utilizing engineered liquid crystalline defect networks. Nat Commun. 2015;6:7180.

[29] Wang M, Li Y, Yokoyama H. Artificial web of disclination lines in nematic liquid crystals. Nat Commun. 2017;8:388.

[30] Guo Y, Jiang M, Afghah S, et al. Photopatterned Designer Disclination Networks in Nematic Liquid Crystals. Adv Opt Mater. 2021;9:2100181.

[31] Guo Y, Jiang M, Peng C, et al. High-Resolution and High-Throughput Plasmonic Photopatterning of Complex Molecular Orientations in Liquid Crystals. Adv Mat. 2016;28:2353–2358.

[32] Jiang M, Guo Y, Yu H, et al. Low f-Number Diffraction-Limited Pancharatnam–Berry Microlenses Enabled by Plasmonic Photopatterning of Liquid Crystal Polymers. Adv Mat. 2019;31:1808028.

[33] Yu H, Jiang M, Guo Y, et al. Plasmonic Metasurfaces with High UV–Vis Transmittance for Photopatterning of Designer Molecular Orientations. Adv Opt Mater. 2019;7:1900117.

[34] Kasyanyuk D, Pagliusi P, Mazzulla A, et al. Light manipulation of nanoparticles in arrays of topological defects. Sci Rep. 2016;6:20742.

[35] Jiang J, Ranabhat K, Wang X, et al. Active transformations of topological structures in light-driven nematic disclination networks. Proc Natl Acad Sci U S A. 2022;119:32122226119.

[36] Harkai S, Murray BS, Rosenblatt C, et al. Electric field driven reconfigurable multistable topological defect patterns. Phys Rev Res. 2020;2:013176.

[37] Nys I, Berteloot B, Beeckman J, et al. Nematic Liquid Crystal Disclination Lines Driven by A Photoaligned Defect Grid. Adv Opt Mater. 2022;10:2101626.

[38] Tkalec U, Ravnik M, Copar S, et al. Reconfigurable knots and links in chiral nematic colloids. Science. 2011;333:62–65.

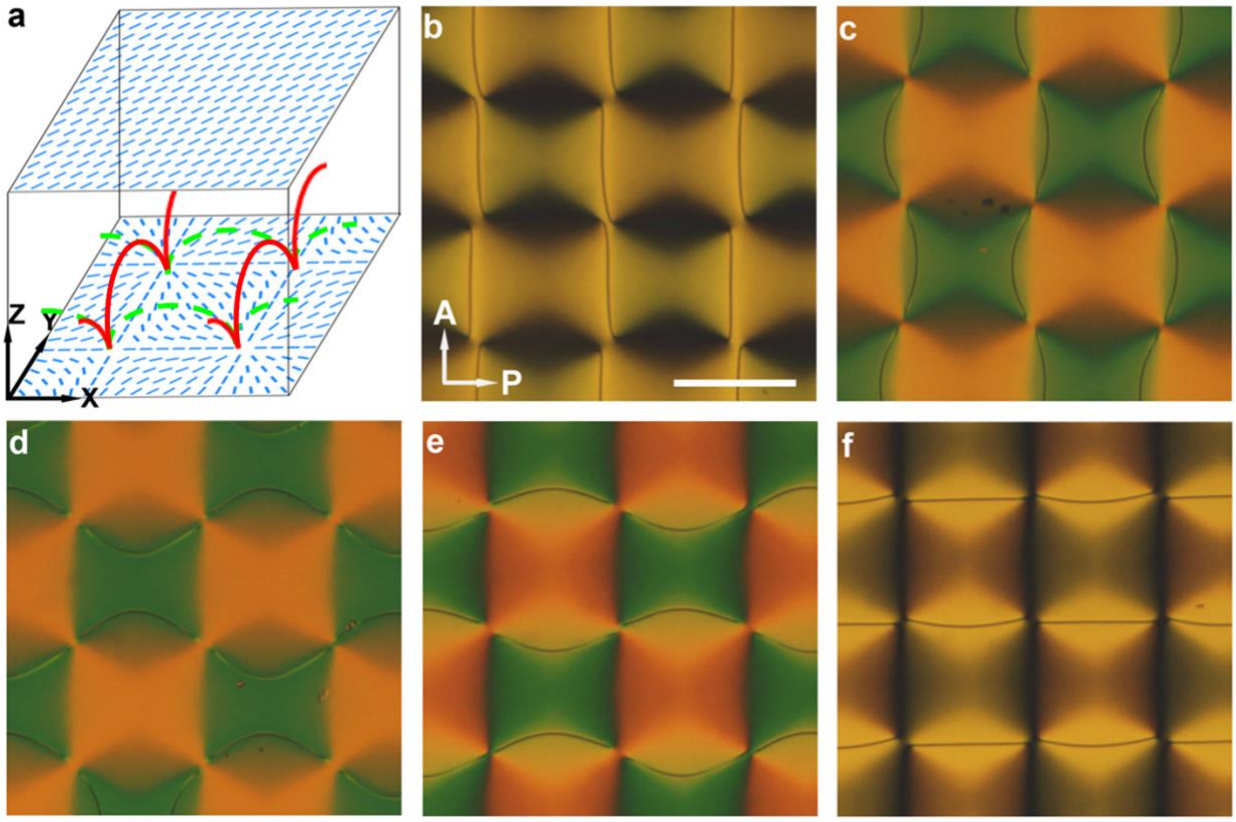

Figure 1. Disclination interconnects generated with ± 1 defect arrays on the bottom surfaces. (a) Schematic of the liquid crystal cell. Red lines and dotted green lines represent two connection modes of disclinations, strengths of all the discliantions are $\pm 1/2$. (b-f) Cross polarized microscope images of the liquid crystal cells with top surface alignment corresponding to θ=0° (b), θ=30° (c), θ=45° (d), θ=60° (e), and θ=90° (f). Scale bar in (b) is 100 μm.

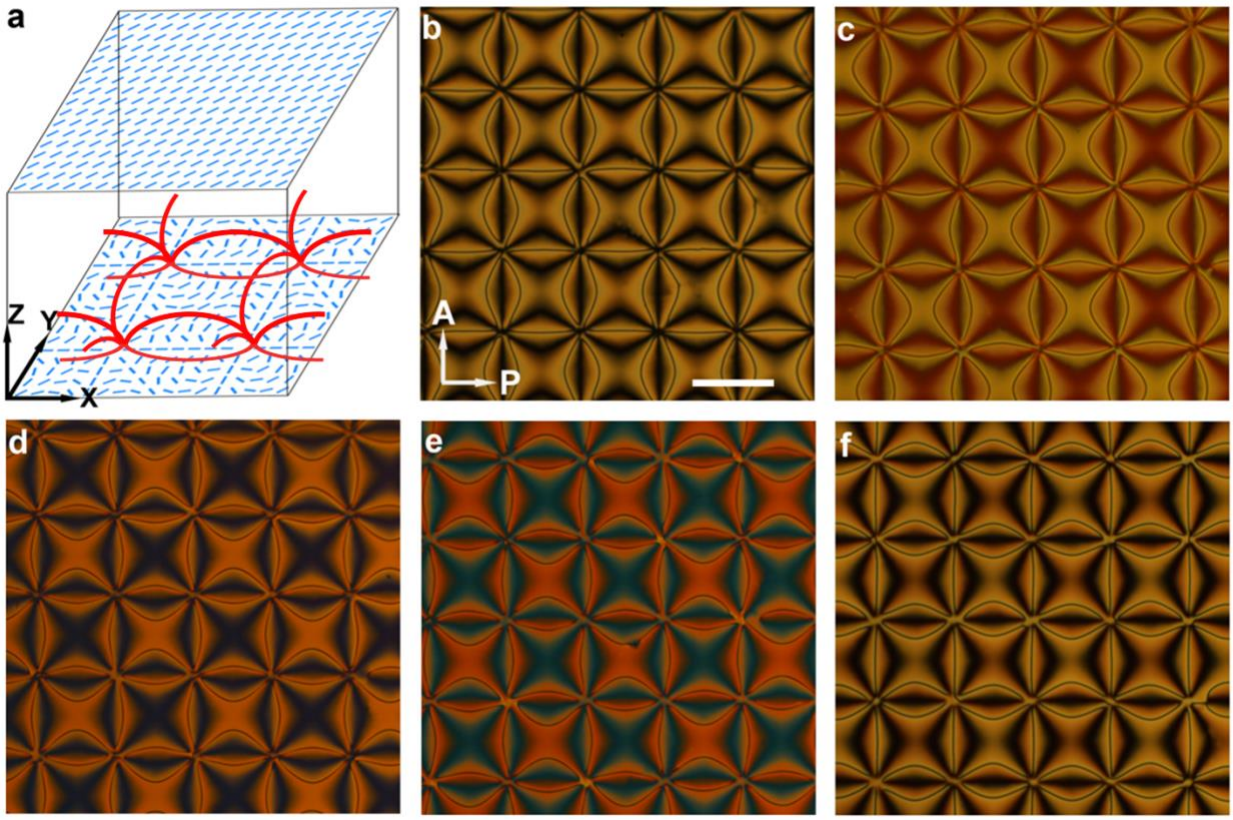

Figure 2. Disclination interconnects generated with ± 3 defect arrays on the bottom surface, strengths of all the discliantions are $\pm 1/2$. (a) Schematic of liquid crystal cell. Red lines represent one connection mode of disclinations. (b-f) Cross polarized microscope images of liquid crystal cells with top surface alignment corresponding to θ=0° (b), θ=30° (c), θ=45° (d), θ=60° (e), and θ=90° (f). Scale bar in (b) is 100μm.

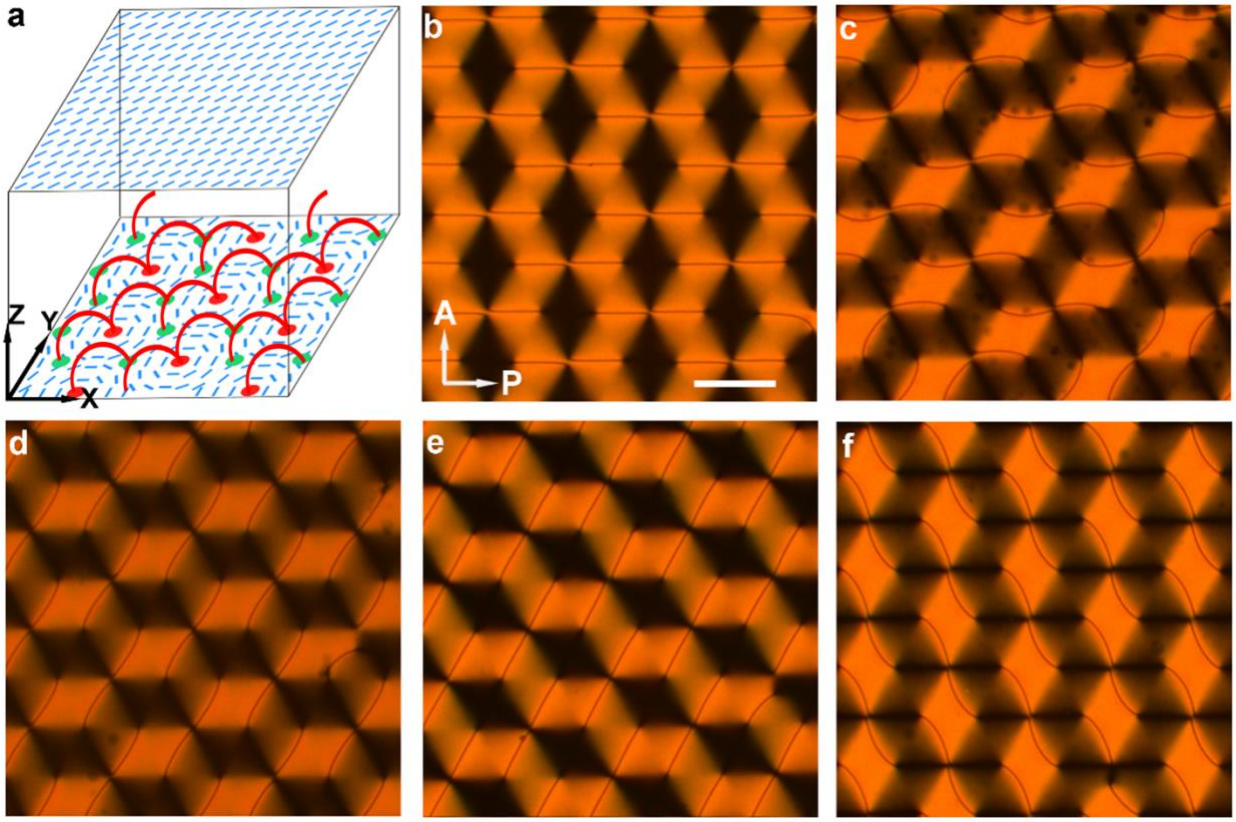

Figure 3. Disclination interconnects generated with a hexagonal defect pattern on the bottom surface. (a) Schematic of liquid crystal cell. Red spots represent +1 defect centers, green spots represent -1/2 defect centers, and red lines represent one connection mode of disclinations. (b-f) Cross polarized microscope images of liquid crystal cells with top surface alignment corresponding to $\theta=0°$ (b), $\theta=30°$ (c), $\theta=45°$ (d), $\theta=60°$ (e), and $\theta=90°$ (f). Scale bar in (b) is 100μm.

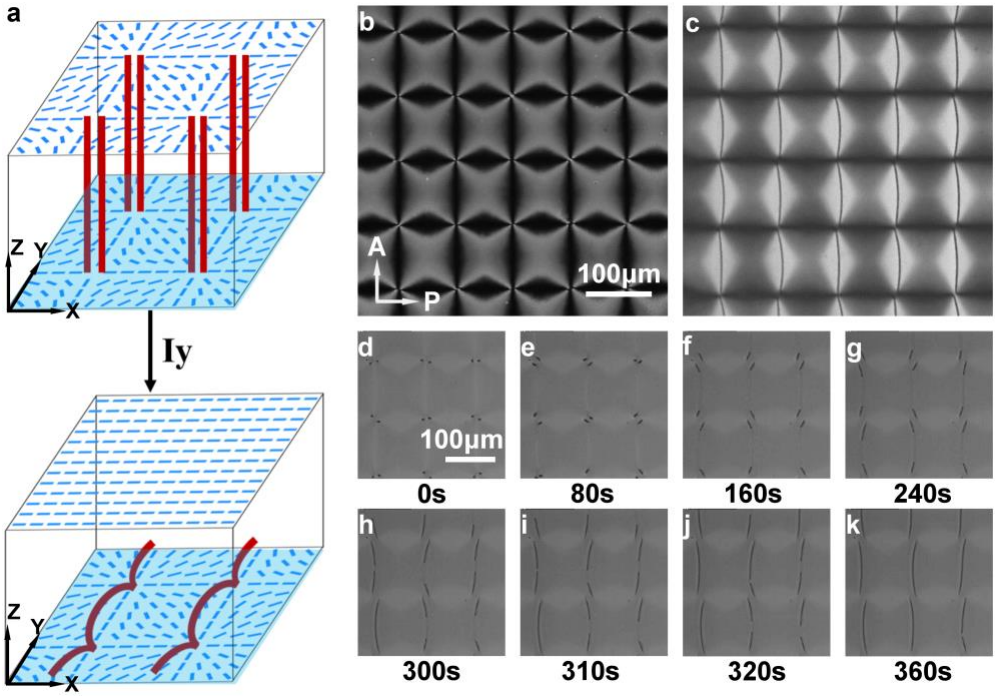

Figure 4. Switching disclination interconnecting two surfaces to one surface. (a) Schematic of the liquid crystal cell alignment pattern and disclinations before and after reconfiguration process. I_y represents light with polarization along y-axis. (b, c) Polarizing optical microscopic images of a liquid crystal cell before (b) and after (c) reconfiguration process. (d-k) Evolution of disclinations under bright field microscope during reconfiguration process.

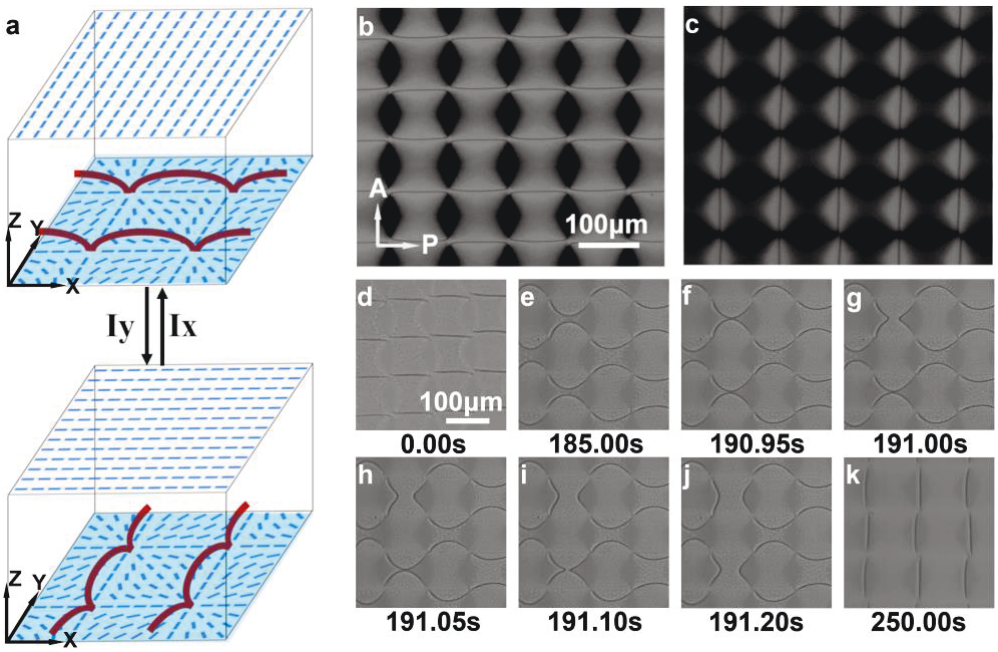

Figure 5. Switching between interconnecting defect centers along different orientations by polarized light. (a) Schematic of the liquid crystal cell alignment pattern and disclinations before and after reconfiguration process. I_x and I_y represents light with polarization along x-axis and y-axis respectively. (b, c) Polarizing optical microscopic images of liquid crystal cell before (b) and after (c) reconfiguration process. (d-k) Evolution of disclinations under bright field microscope during reconfiguration process.

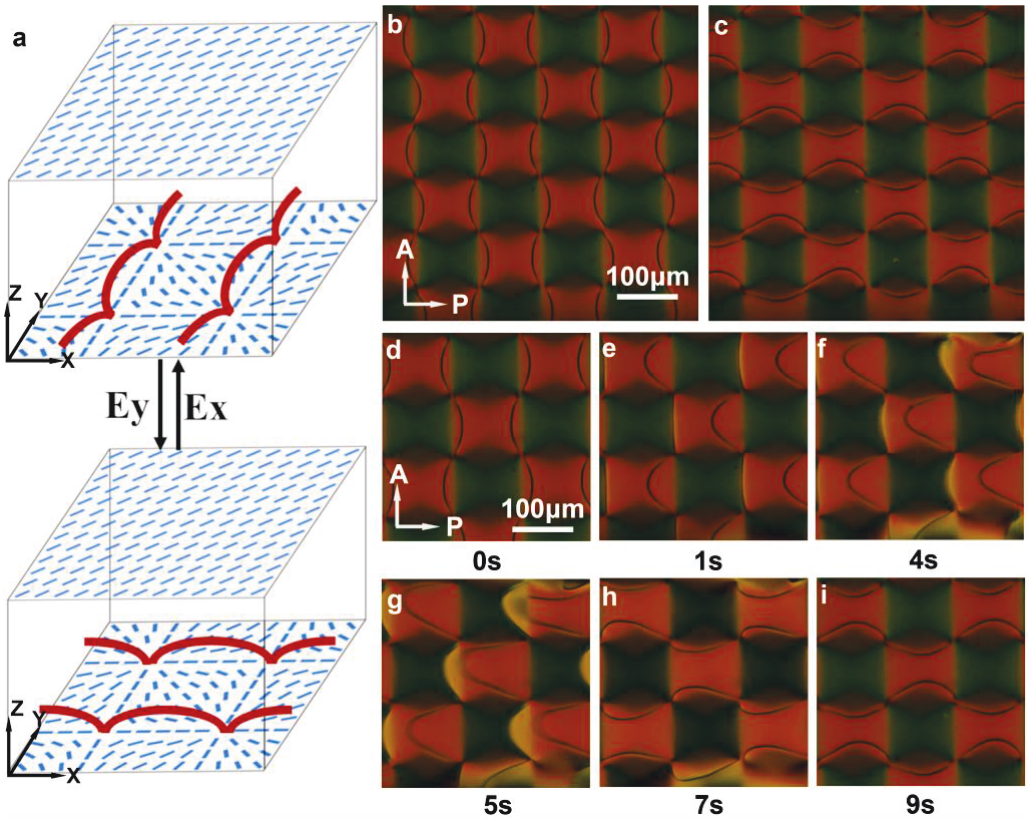

Figure 6. Reconfiguring disclination interconnects between degenerate states with electric field. (a) Schematic of the liquid crystal cell alignment pattern and disclinations before and after reconfiguration process. E_x and E_y represents electric field along x-axis and y-axis respectively. (b, c) Polarizing optical microscope images of liquid crystal cell before (b) and after (c) reconfiguration process. (d-i) Evolution of disclinations under cross-polarized microscope during reconfiguration process.